Research Paper

Dissociation of neonatal and adult mice brain for simultaneous analysis of microglia, astrocytes and infiltrating lymphocytes by flow cytometry

Belén Calvo*, Felipe Rubio, Miriam Fernández, Pedro Tranque

Neuroglia Laboratory, Research Institute for Neurological Disorders (IDINE), Medical School, University of Castilla-La Mancha (UCLM), Albacete, Spain

ARTICLE INFO

ABSTRACT

The technical difficulty to isolate microglia, astrocytes and infiltrating immune cells from mouse brain is nowadays a limiting factor in the study of neuroinflammation. Brain isolation requirements are cell-type and animal-age dependent, but current brain dissociation procedures are poorly standardized. This lack of comprehensive studies hampers the selection of optimized methodologies. Thus, we present here a comparative analysis of dissociation methods and Percoll-based separation to identify the most efficient procedure for the combined isolation of healthy microglia, astrocytes and infiltrated leukocytes; distinguishing neonatal and adult mouse brain. Gentle mechanical dissociation and DNase I incubation was supplemented with papain or collagenase II. Dispase II digestion was also used alone or in combination. In addition, cell separation efficiency of 30 % and 30–70 % Percoll gradients was compared. In these experiments, cell yield and integrity of freshly dissociated cells was measured by flow cytometry. We found that papain digestion in combination with dispase II followed by 30 % Percoll separation is the most balanced method to obtain a mixture of microglia, astrocytes and infiltrated immune cells; while addition of dispase II was not an advantage for neonatal brain. These dissociation conditions allowed flow cytometry detection of a slight glial activation triggered by sublethal LPS injection. In conclusion, the enzymes and Percoll density gradients tested here affected differently resting microglia, activated microglia/macrophages, astrocytes and infiltrated lymphocytes. Also, newborn and adult brain showed contrasting reactions to digestion. Our study highlights the strength of flow cytometry for the simultaneous analysis of neuroimmune cell populations once extraction is optimized.

1. Introduction

Brain microglia and astrocytes play critical roles in brain injury and neuroinflammation. Activation of these glial cells together with leukocyte infiltration in the CNS contribute to modulate neuronal survival in a number of neuropathologies (Bergmann et al., 1999). *In vitro* models such as cultures of glial cell lines, primary astrocytes and primary microglia have been extensively used to investigate the role of specific brain cells, helping to identify factors involved in neuroimmunity (Guttenplan and Liddelow, 2019; Moussaud and Draheim, 2010; Singh et al., 2014). Nevertheless, these models fail to mimic the complexity of cellular interactions within the brain; and the study of neurodegeneration and brain repair ultimately need to relay on *in vivo*

approaches in which the functional characterization of discrete cell populations is generally more challenging due to the difficulty to isolate brain cells (Guttenplan and Liddelow, 2019; Legroux et al., 2015; Erturk et al., 2016).

Typically, isolation methods for brain immune cells are based on mechanical dissociation alone or in combination with enzymatic digestion. Microglia and astrocytes isolated from brain can be grown as mixed cultures, and further separated by mild trypsinization and shaking (McCarthy and De Vellis, 1980; Saura et al., 2003). However, separation protocols that are appropriate for cells in culture are generally not so efficient for dissociation of brain cells, since these are much more intermingled. In this regard, brain tissue digestion from adult mice is especially challenging, and a large number of enzymatic

* Corresponding author.
E-mail addresses: belen.crodriguez@uclm.es (B. Calvo), felipe.rubio1@alu.uclm.es (F. Rubio), miriam.fernandez@uclm.es (M. Fernández), pedro.tranque@uclm.es (P. Tranque).

procedures have been developed with the goal to extract cells from brain with a high yield, while preserving integrity. Enzymes such as papain, collagenase II and dispase II are among the most recommended for brain dissociation (Moussaud and Draheim, 2010; Swartzlander et al., 2018; Sedgwick et al., 1991; Cardona et al., 2006; Lee and Tansey, 2013; Stevens et al., 2002). Unfortunately, the existing literature presents substantial limitations in providing a comprehensive analysis that enables comparison of the different procedures in terms of cell yield, purity or integrity. Comparative studies are needed to facilitate the choice of dissociation protocols that are effective for specific cell types and adapted to brain age.

Percoll density gradients following enzymatic dissociation are extensively used to separate specific cell subpopulations from brain tissue homogenates (Legroux et al., 2015; Bergmann et al., 1999; Moussaud and Draheim, 2010). Percoll gradients have proven useful for separation of microglia (Ponomarev et al., 2005; Sedgwick et al., 1991), astrocytes and lymphocytes (Batiuk et al., 2017; Bergmann et al., 1999); but also for other brain cell types such as neurons and oligodendrocytes (Guez-Barber et al., 2012; Legroux et al., 2015), as well as synaptosomes and other organelles (Thorne et al., 1991). Moreover, complementing density gradients with methods based on the use of antibodies for the detection of specific cell surface markers has improved the separation and analysis of microglia, astrocytes, and other neural cells. Among these procedures, those based on flow cytometry are the most-frequently used (Legroux et al., 2015; Erturk et al., 2016; Bruttger et al., 2015; Czupalla et al., 2018); although magnetic bead separation (Bedi et al., 2013) and immunopanning (Zhang et al., 2016) have also been found suitable for certain brain cell types, specially microglia cells. Flow cytometry is nowadays a powerful tool for analyzing cellular immune responses, and a useful technique for identifying molecular changes in individual cell types within the brain. Moreover, flow cytometry provides clear benefits in terms of data quantitation and sample throughput compared to alternative methods such as immunohistochemistry and *in situ* hybridization (Sedgwick et al., 1991; Stevens et al., 2002; Bedi et al., 2013; Jungblut et al., 2012). Fluorescence-activated cell sorting (FACS) is also a flow cytometry-based technique especially attractive for the study of neuroinflammation, as it has been shown effective to separate precursor cells from immature brain (Maric and Barker, 2005) as well as adult brain neurons (Guez-Barber et al., 2012) and microglia (Sierra et al., 2007). However, application of these flow cytometry techniques to neuroscience is modest compared to its expansion in immunology and cancer studies. This is mostly due to the difficulty to dissociate brain tissue and obtain intact single cells.

Here we carry out a comparative analysis of cell isolation methods to find optimal conditions for the simultaneous evaluation of microglia, astrocytes and lymphocytes by flow cytometry, distinguishing between neonatal and adult brain. Neural tissue was treated with different enzymatic cocktails in combination with gentle mechanical dissociation. In addition, two alternative Percoll gradient densities were examined for cell separation. Overall, we detected remarkable differences between neonatal and adult brain tissue in terms of enzyme performance.

Finally, our optimized method for dissociation of adult brain combined with flow cytometry was found suitable to detect mild glial cell activation in mice injected with a sublethal dose of lipopolysaccharide (LPS).

2. Experimental procedure

2.1. Animals

Wild-type C57BL/6 J mice were housed in the facilities associated to Albacete Medical School in a 12 h light/dark cycle. Food and water were supplied ad libitum. Neonate mice between 5–7 days and adult mice between 4–6 months were used for experiments. All procedures related to animal use and care were approved by the Ethics Committee for Animal Experimentation of the University of Castilla- La Mancha.

2.2. LPS administration

To assess the functional status of microglia and astrocytes after stimulation of immunity, mice received an intraperitoneal injection (i.p.) of 0.5 mg/kg LPS (LPS powder was dissolved in sterile endotoxin-free 0.9 % saline at a concentration of 10 mg/ml, *Salmonella enterica*, serotype *typhimurium*, L7261 Sigma-Aldrich). Three days after treatment mice were euthanized, and brains were removed for immunohistochemistry or flow cytometry analysis of glial cells.

2.3. Cell dissociation

C57 mice were euthanized *via* cervical dislocation and decapitated. Brains were extracted and placed in cold Hank's Balanced Salt Solution (Gibco 14175) without calcium chloride or magnesium chloride (HBSS [-]CaCl$_2$/[-]MgCl$_2$) after removal of cerebellum and olfactory bulbs. Meninges, blood vessels and choroid plexus were carefully separated; and tissue was finely minced with a scalpel prior to digestion.

Chopped brain tissue was placed in MACS C tubes (Miltenyi Biotec 130-093-237) in a total volume of 5 ml and processed with a mechanic dissociator at 6 rpm for 30 min. Non enzymatic dissociation was carried out in Earle's Balanced Salt Solution (EBSS [+]CaCl$_2$/[+]MgSO$_4$, Gibco 24010). Enzymatic dissociation was performed with papain (100 U, Worthington LK003178) in EBSS; collagenase II (600 U, Millipore 234155) in 1X HBSS with 90 mM Ca$_2$+, dispase II in EBSS (6 U, Sigma-Aldrich D4963); or combinations of papain and dispase II, or colagenase II and dispase II. DNAse I (100 U, Sigma-aldrich DN25) was added to all solutions. Prior to use, papain was activated for 30 min at 37 °C and 5 % CO2. To stop all digestions, samples were diluted with cold HBSS and placed on ice. Solutions were then further homogenated for 10 times using a 5 ml pipette and filtered through a 70 μm cell strainer (BD 352350). The resulting single cell suspension was centrifuged at 300g for 10 min at RT.

Percoll™ (GE Healthcare 17-0891-01) gradients were used to remove myelin and enrich the homogenate for viable glial cells. A stock solution of isotonic Percoll (SIP) was prepared (9:1 Percoll in 10x HBSS [-]CaCl$_2$/[-]MgCl$_2$, Gibco 14185). Cell pellets were resuspended in a 30 % (v/v) or 30–70 % (v/v) SIP (in 1x HBSS). For the 30 % Percoll gradient, 3 ml of SIP were added to 7 ml of 1X HBSS containing the cell suspension in a 14 ml polypropylene tube. In turn, the 30–70 % Percoll gradient was performed by placing 3 ml of 70 % SIP diluted with 1x HBSS in a 14 ml tube; which was overlaid with 10 ml of 30 % SIP containing the cell suspension. Gradients were centrifuged without brake for at 300g 30 min at 18 °C. After centrifugation, cells were collected from the bottom layer in the 30 % Percoll gradient, or the middle layer (4 ml interphase) in the 30–70 % Percoll gradient. For both types of Percoll centrifugations, cells were washed by adding 1X HBSS, centrifugated for 10 min at 300 g, and resuspended in 10 ml of 1X red blood cell lysis buffer (1:10 from 10x red blood cell lysis solution in sterile non-deionized distilled H$_2$O, Miltenyi Biotec 130-094-183) at 4 °C. Solutions were centrifuged at 300g for 10 min and cell pellets were finally resuspended in 50 μl of blocking buffer consisting in 1X PBS, 0.5 % albumin from bovine serum (BSA, Sigma-Aldrich A7906) and 2 mM ethylenediaminetetraacetic acid tetrasodium salt dihydrate (EDTA, Sigma-Aldrich E6511) before flow cytometry staining (Fig. 1).

2.4. Flow cytometry

Flow cytometry staining was performed at 4 °C. To block surface antigens in microglial cells or macrophages, 0.5 μl of *FcR Blocking Reagentfor mouse* (1:100 dilution, Miltenyi Biotec 130-059-901) was added to the blocking buffer containing the cell suspension and incubated for 10 min. Subsequently, a mix containing fluorochrome-conjugated antibodies recognizing mouse CD45, CD11b, ACSA-1,
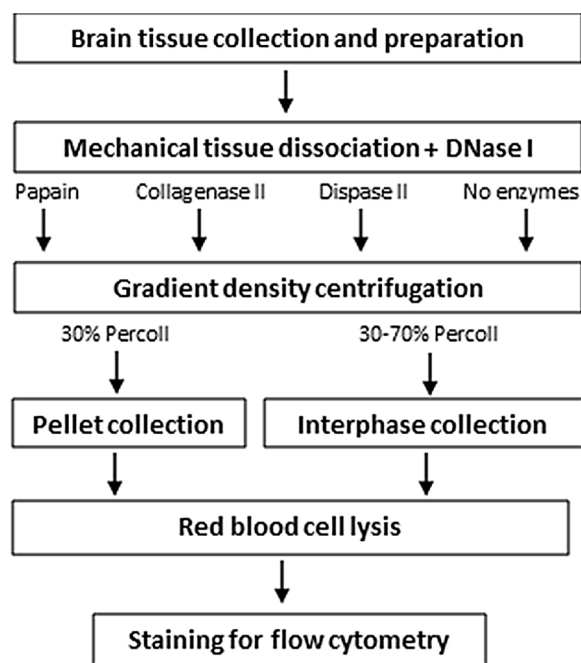
Fig. 1. Workflow outlining the different steps followed in this protocol.

ACSA-2 (1:11 to 1:20 dilution). To determine cell death, DAPI was added and incubated for 10 min (Table 1). The DAPI concentration used (1 μg/ml) was appropriate to distinguish live and dead cells (Gordon et al., 2003). Samples were washed with 1 ml of blocking buffer and centrifugated for 5 min at 300g. Finally, cell pellets were resuspended in 500 μl of PBS and samples were immediately used for flow cytometry. Fluorescent calibration beads (1000 beads/μl) were added for counting the absolute number of cells. Data were acquired using a MACSQuant flow cytometer and analyzed with the MACSQuantify software (Miltenyi Biotec).

2.5. Immunohistochemistry

Mice were deeply anesthetized and intracardially perfused with saline 0.9 % (w/v). Brains were collected and post-fixed with 4 % paraformaldehide for 24 h. After post-fixation, they were cryoprotected with 30 % sucrose and frozen at −20 °C until sectioning. Sections (20 μm) were cut using a cryostat (Microm™ HM550, ThermoFisher), thaw-mounted onto Superfrost Plus slides (ThermoFisher J1800AMNZ) and finally stored at −20 °C until staining.

Sections were used for double-label immunohistochemistry staining as previously described (Serrano-Perez et al., 2011). Both the primary and secondary antibody solutions were diluted in 1X PBS containing 1 % BSA. Sections were incubated with primary antibodies anti-rabbit Iba-1 (1:500 dilution, Wako Chemicals 019-19741) and anti-mouse

GFAP (1:500 dilution, Sigma-Aldrich G6171). Alexa Fluor 488-conjugated goat anti-rabbit IgG (1:2000 dilution, ThermoFisher A11031) and Alexa Fluor 568-conjugated goat anti-mouse IgG (1:2000 dilution, ThermoFisher A11008) were used as respective secondary antibodies. Finally, sections were incubated with DAPI (1 μg/ml) to stain cell nuclei. Appropriate positive control tissue as well as primary- or secondary-only negative controls were also included. Images of the fluorescent labeling were acquired using a ZEISS Apotome.2 microscope with an axiocam 503 mono digital camera and Zen Blue control software version 2.3 (Carl Zeiss). To visualize hippocampal fields, a 10X objective (Plan-APOCHROMAT, V10X, NA 0.45, AIR) was used.

2.6. Statistical analysis

Data were analyzed with GraphPad Prism software (San Diego, CA). Results are represented as mean ± standard error of the mean (SEM) with generally n = 4–6 individual animals. To compare two groups (30 % *vs*. 30–70 % Percoll gradient; or control *vs*. LPS injected mice) we used an unpaired Student *t*-test. For comparison of different digestion protocols, we used a one-way analysis of variance (ANOVA) and a Tukey post-test analysis. Values were considered statistically significant when probability (*p*) values were equal or below 0.05 (*), 0.01 (**), or 0.001 (***).

3. Results

### 3.1. Characterization of brain populations by flow cytometry

In order to compare the efficiency of different dissociation protocols to extract microglia, astrocytes and infiltrated immune cells from mouse brain, we first validated the specificity of the cell cytometry markers and gating strategies used across our study. In these experiments, brains cells were isolated following a common method based on digestion with papain, dispase II and DNase I, followed by a 30 % Percoll density gradient.

Identification of resting microglia as CD11b+/CD45low cells, activated microglia/macrophages as CD11b+/CD45high cells, and lymphocytes as a CD11b-/CD45+ population from adult brain was supported by an extensive literature (Campanella et al., 2002; Stevens et al., 2002; Marques et al., 2008). Moreover, gating of activated microglia/ macrophages was further sustained by incubation with microglia/macrophages activation markers CD206 and CD38 (Jablonski et al., 2015; Hellström Erkenstam et al., 2016). These markers labelled a substantial number of cells within the activated microglia/macrophages gate (32.5 and 42.7 %, respectively), while they were absent from the population identified as resting microglia. In respect to lymphocyte gating, it was verified by CD3 staining of T cells. As expected from previous literature (Posel et al., 2016) we found 23.7 % of T cells within the population of cells gated as lymphocytes (Fig. 2B).

Meanwhile, astrocytes from neonate brains were mechanically extracted, purified with 30 % Percoll and labelled with surface antigens

Table 1
Antibodies and reagents used for flow cytometry analysis.

| Antibody/reagent	Clone	Cell targets	Concentration	Company (reference)
ACSA-1-PE (anti-GLAST)	ACSA-1	Neonatal astrocytes and radial glia	1:25	Miltenyi Biotec (130-118-483)
ACSA-2-APC	IH3-18A3	Neonatal and adult astrocytes	1:25	Miltenyi Biotec (130-117-535)
FcR Blocking Reagent			1:100	Miltenyi Biotec (130-092-575)
Calibration Beads			1000 beads/ml	Miltenyi Biotec (130-093-607)
CD11b-PE Vio770	REA592	Macrophages, microglía, granulocytes, NK cells and subsets of dendritic cells	1:50	Miltenyi Biotec (130-113-246)
CD206-APC Vio770	C068C2	Dendritic cells and subets of macrophages and microglia	1:10	BioLegend (141708)
DAPI (VioBlue gate)		Dead cells	1 μg/ml	Sigma-Aldrich (D9542)
CD3-APC	REA641	T cells	1:25	Miltenyi Biotec (130-122-943)
CD38-APC	REA616	Subsets of macrophages, microglía, B cells and T cells	1:10	Miltenyi Biotec (130-109-259)
CD45-PE	30F11	Hematopoietic cells except erythrocytes	1:25	Miltenyi Biotec (130-117-498)
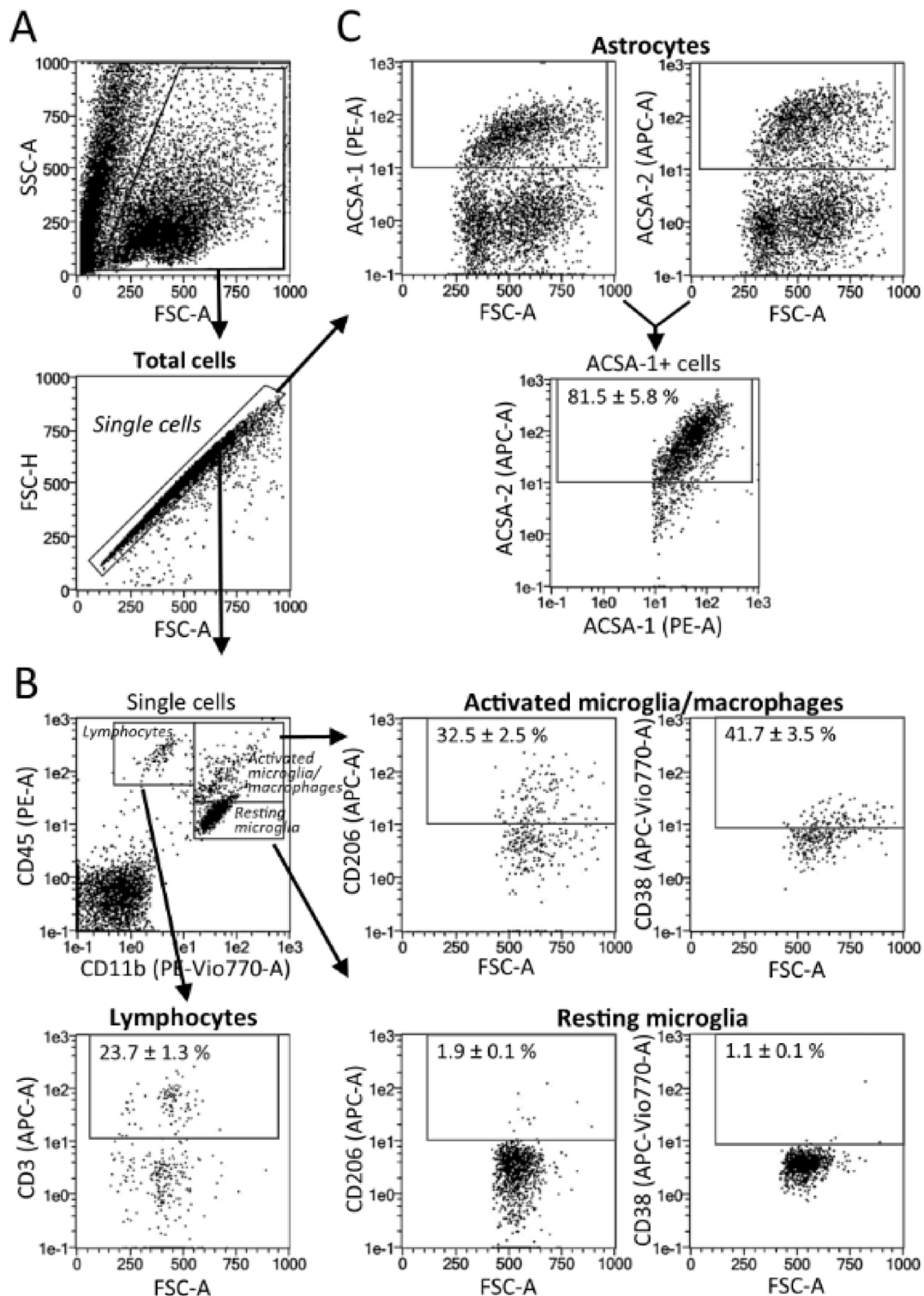
Fig. 2. Cell cytometry markers and gating strategy for the analysis of brain cell populations. Neural cells were isolated from mouse and further purified using 30 % Percoll. (A) Gates to exclude debris and cell aggregates in FSC-A/SSC-A and FSC-A/FSC-H plots. (B) Single cells from adult brain were obtained with papain and dispase II. Gates correspond to resting microglia (CD11b+/CD45^{low}), activated microglia/macrophages (CD11b+/CD45^{high}) and lymphocytes (CD11b-/CD45+). Activated microglia/ macrophage gating was further sustained by incubation with microglia/macrophage activation markers CD206 and CD38; while lymphocyte gating was verified by CD3 staining of T cells. (C) Gates for ACSA-1+ and ACSA-2+ astrocytes extracted from neonatal brain, showing extensive staining overlapping. Numerical values correspond to mean ± S.E.M (n = 4).

ACSA-1 and ACSA-2, previously validated as specific markers for astrocytes (Kantzer et al., 2017). According to our results (Fig. 2C), expression of these antigens highly overlaps when analyzed by flow cytometry after double staining (81,5 % of ACSA-1 astrocytes show ACSA-2 staining). Since ACSA-1 staining has been reported to decrease, while ACSA-2 is preserved in adult astrocytes (Furuta et al., 1997; Regan et al., 2007), ACSA-2 was the astrocyte marker of choice for our next experiments.
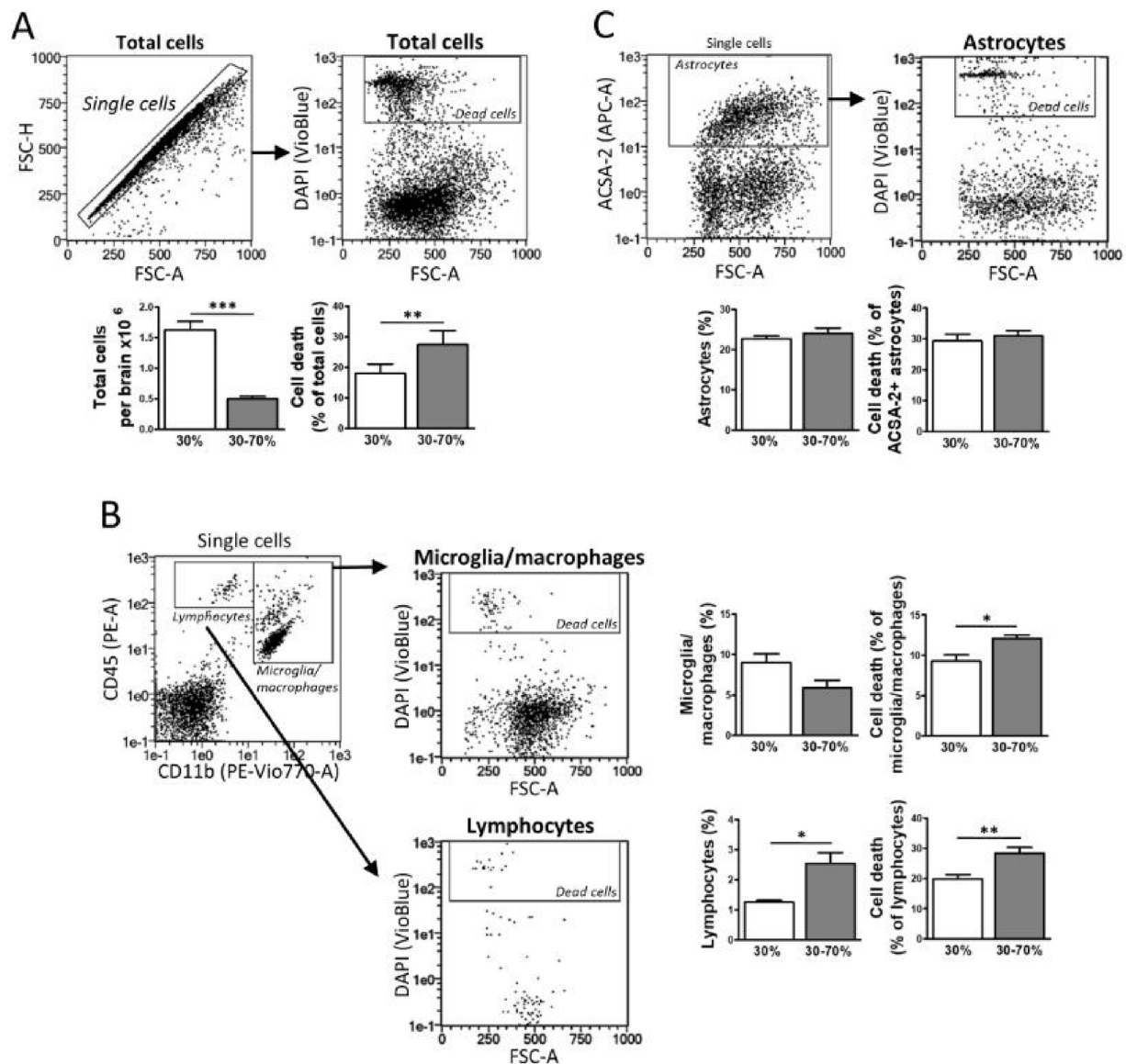
Fig. 3. Comparison of Percoll density gradients for flow cytometry analysis of brain cell recovery. Neural cells were isolated from adult brain by enzymatic dissociation followed by comparison of 30 % and 30–70 % Percoll density gradients to separate cells from myelin and debris. DAPI staining of dead cells was applied to the analysis of total cells (A), CD11b + /CD45 + microglia/macrophages (B), CD11b-/CD45 + lymphocytes (B), and ACSA-2 + astrocytes (C). Graphs show cell recovery as well as the fraction of dead cells (%) for each brain population, comparing values after 30 % and 30–70 % Percoll purification. Data represent mean ± S.E.M. (n = 5–6). *, p < 0.05; **, p < 0.01; ***, p < 0.001.

3.2. Selection of Percoll gradient

Percoll density gradients are frequently used after mechanical or enzymatic digestion during cell isolation. These gradients not only contribute to separation according to cell size, but also to efficient removal of myelin and cellular fragments (Lee and Tansey, 2013; Ni and Aschner, 2010). However, gradients need to be optimized to present an adequate balance between cell yield and loss of viability. So, before comparing alternative enzymatic digestion we tested 30 % *vs*. 30–70 %, as these two Percoll gradients are commonly used to separate microglia and astrocytes. The 30 % Percoll gradient removes myelin, driving all cells to the pellet; whereas 30–70 % Percoll provides higher purity as it separates glial cells from other cell types. Adult brain tissue was subjected to a standard enzymatic digestion with papain, dispase II and DNase I, and the resulting cell suspension was applied to either a 30 % or 30–70 % Percoll gradient. Total cell recovery and survival were determined by flow cytometry following the gating strategies depictured in Fig. 3. Results indicate that 30 % Percoll triplicates the

number of total cells obtained (1.6 × 106 per brain) with respect to 30–70 % gradients; while the DAPI staining corresponding to total dead cells is significantly lower (Fig. 3A). Percoll gradient choice did not influenced microglia recovery, although fewer lymphocytes were obtained with 30 % Percoll. We also found that both microglia/macrophage and lymphocyte death was significantly lower with 30 % Percoll (Fig. 3B). Regarding the astrocyte population, there were no differences in extraction and viability among gradients (Fig. 3C). Therefore, according to these data, 30 % Percoll stands out in terms of cell yield and viability in our experimental conditions.

3.3. Total neural cell yield and viability as a result of enzymatic digestion

After selecting the 30 % Percoll gradient for our following studies, alternative enzymatic digestions were compared. We evaluated by flow cytometry the total neural cells obtained when mechanical dissociation is combined with several enzymes that have been previously used for the extraction of functional glial populations, such as papain,
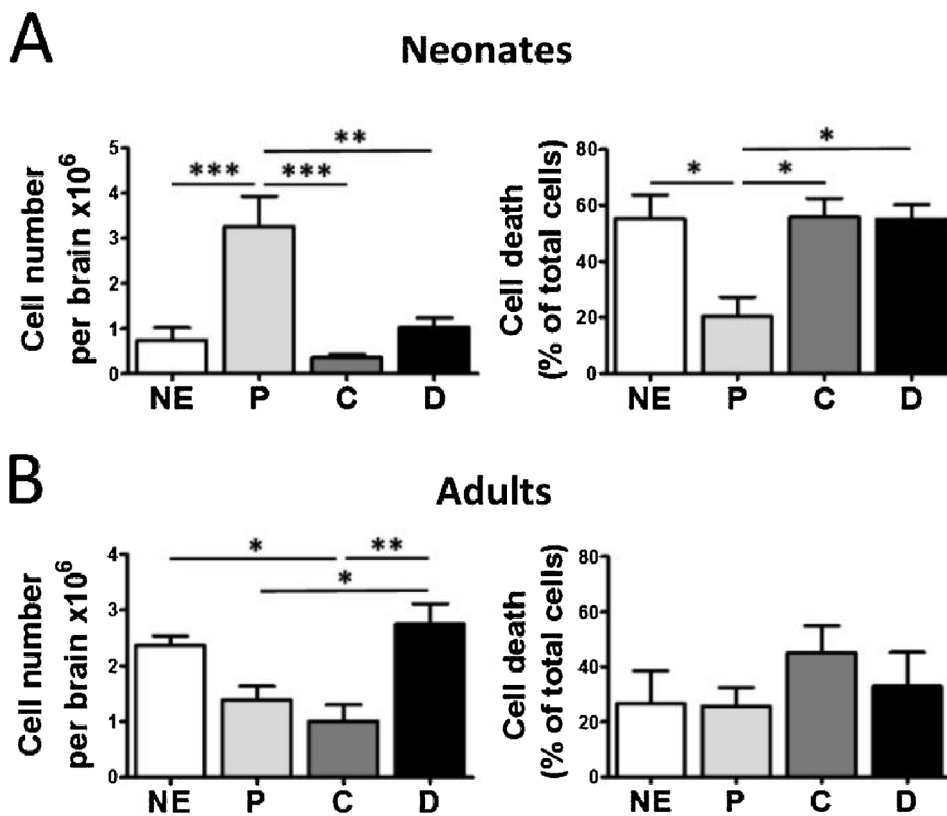
Fig. 4. Enzymatic digestion conditions neural cell recovery from neonate and adult brains. Neonatal (A) or adult brains (B) were digested with papain (P), collagenase II (C), dispase II (D) or non-enzymatically (NE), all in combination with DNase I and gentle mechanical dispersion. After enrichment using a 30 % Percoll gradient, the isolated cells were processed for flow cytometry analysis of total cell number. DAPI staining allowed evaluation of cell death. Data are expressed as mean ± S.E.M. (n = 4 for adult and n = 5–6 for neonate experiments). *, p < 0.05; **, p < 0.01; ***, p < 0.001.

collagenase II and dispase II. Regarding enzyme concentration, we used 20 U/ml of papain, 120 U/ml of collagenase II and 1.2 U ml of dispase II based on recommendations by different authors to obtain optimal brain tissue dissociation while preserving cell integrity. Thus, papain at 15–23 U/ml has been previously reported to isolate microglia (Moussaud and Draheim, 2010; Singh et al., 2014) and astrocytes (Ben-Gigi et al., 2015; Holt et al., 2019) from adult mice without causing significant cell activation during digestion. Dispase II has also been identified as a gentle enzyme for tissue dissociation and was used for the isolation of viable microglia either alone (2 U/ml) (Boelen et al., 2012) or in combination with papain (1.2 U/ml) (Lee and Tansey, 2013). Collagenase II at 120 U/ml has also been the concentration chosen in several experiments that isolate microglia and astrocytes for their analyses by flow cytometry (Sierra et al., 2007).

Since enzyme requirements for tissue digestion are expected to change with age, we analyzed both P5 neonatal and adult mice brains. Results showed that papain was significantly more efficient for neonate tissue than any other procedure, recovering over 3×10^6 cells per brain (Fig. 4A). Contrarily, non-enzymatic dissociation and dispase II were more effective than papain and collagenase II to disperse adult brain cells (Fig. 4B). These data indicate that cell recovery is highly affected by the dissociation method used, and that requirements for neonatal and adult tissue are different. In addition, DAPI staining after each dissociation procedure showed that papain preserves cell integrity significantly better than any other enzyme in neonates, but not in adults (Fig. 4A and B). In conclusion, animal age is a critical factor for the efficient isolation of healthy cells from brain.

3.4. Recovery of resting microglia, activated microglia/macrophages and lymphocytes from neonatal and adult mouse brain

Discrete cell types within the brain are expected to show individual responses to dissociation. Thus, our next set of experiments specifically assessed the impact of dissociation methods on the recovery of myeloid and lymphoid cells. Tissue from newborn as well as adult mice was

obtained as described before. After 30 % Percoll-gradient purification, cell suspensions were stained with specific markers for resting microglia (CD11b+/CD45^{low}), activated microglia together with other macrophages (CD11b+/CD45^{high}), and lymphocytes (CD11b-/CD45+). Flow cytometry analysis revealed that collagenase II is the most advantageous enzyme to extract all these cell populations from newborn brain (Fig. 5A). However, despite the high extraction yields obtained with collagenase II, flow cytometry analysis of cell survival after DAPI staining showed that papain digestion preserves viability of resting microglia in newborn tissue better than collagenase II. Regarding adult tissue, collagenase II and papain are generally more effective than dispase II or no-enzymatic methods to extract resting microglia, activated microglia/macrophages and lymphocytes. Moreover, all procedures showed similar lethality for resting microglia (Fig. 5B). We conclude from these experiments that the choice of enzymes for digestion greatly affects microglia/macrophage and lymphocyte recovery, and the age of animals is a key factor to consider.

3.5. Analysis of dissociation methods for the extraction of brain astrocytes

We used ACSA-2 as astrocyte specific marker to evaluate astrocyte recovery in both newborn and adult brain (Batiuk et al., 2017; Jungblut et al., 2012). Data collected show that the different enzymatic digestions used do not improve mechanical extraction of astrocytes. In fact, enzymes generally have a negative effect on astrocyte recovery, especially when acting on adult brain (Fig. 6).

To check whether differences in astrocyte recovery are related to differential effects of enzymes on cell viability, we analyzed by flow cytometry the DAPI labelling of ACSA-2+ astrocytes. Our results indicate once again that mechanical dissociation is generally more effective than enzymatic procedures to maintain cell viability. Besides, collagenase II was the most deleterious enzyme for ACSA-2 astrocytes in neonatal tissue (Fig. 6A); whereas papain showed the highest death values within adult astrocytes (Fig. 6B). These observations underline the notion that mice age determines tissue sensitivity to enzymes.
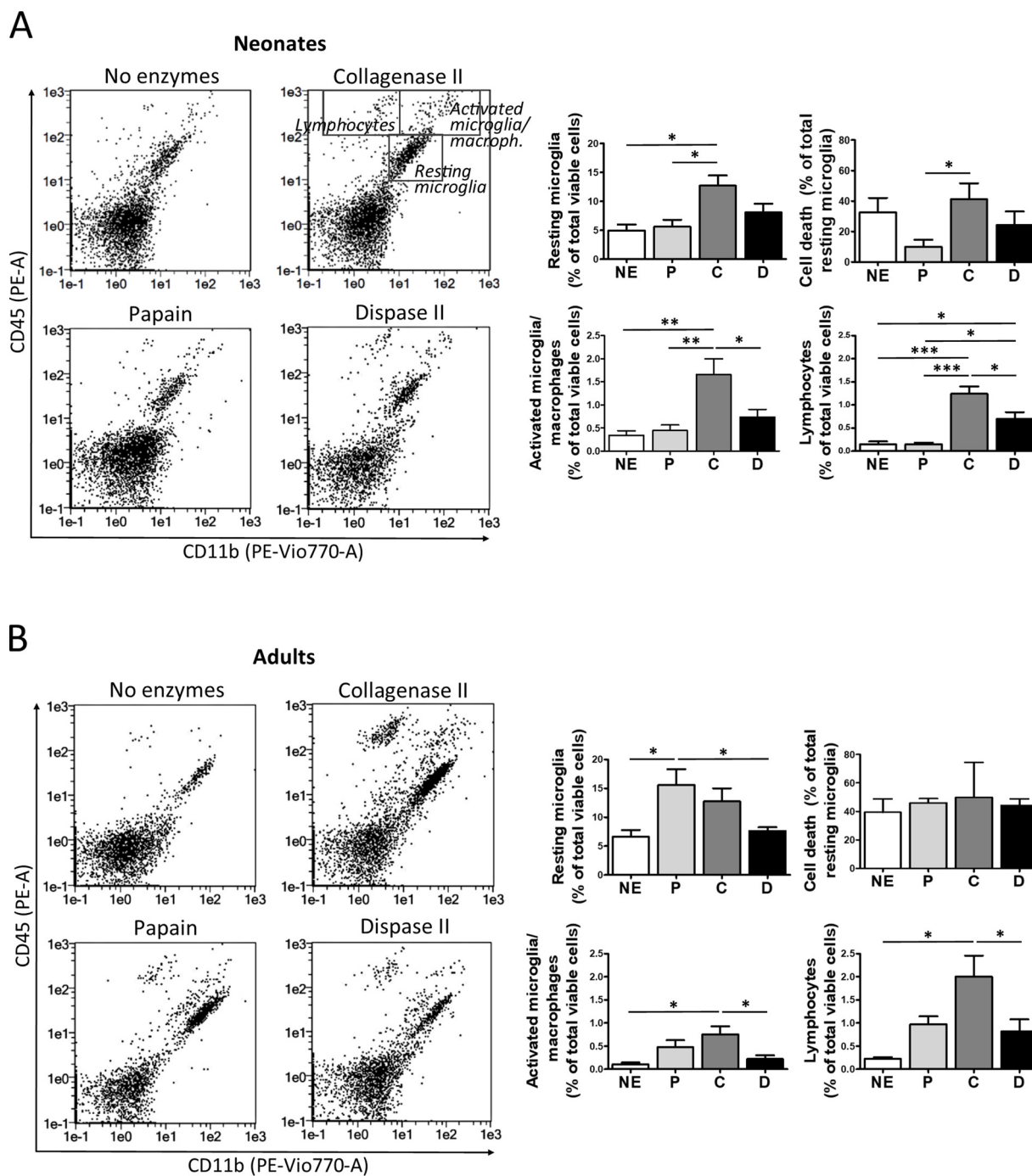
Fig. 5. Recovery of myeloid and lymphoid cells from newborn and adult mice brains. Tissue from neonatal (A) and adult brain (B) was mechanically dissociated while digested with papain (P), collagenase II (C), dispase II (D) or in the absence of enzymes (NE); and brain homogenates were stained for flow cytometry analysis. Representative plots for each isolation protocol are included. Gates drawn correspond to resting microglia (CD11b+/CD45^{low}), activated microglia/macrophages (CD11b+/CD45^{high}), and lymphocytes (CD11b-/CD45+). Cell death within resting microglia was measured after DAPI staining. Associated graphs correspond to % of each population and resting microglia death. Values in all graphs are expressed as percentage of total cells and represent mean ± S.E.M. (n = 4–5). *, $p < 0.05$; **, $p < 0.01$; ***, $p < 0.001$.

3.6. Effects of dispase II addition on neural cell recovery and viability

Dispase II is a neutral protease with mild effects on brain tissue, frequently used in combination with other enzymes (Lee and Tansey, 2013; Ni and Aschner, 2010). Accordingly, to examine the ability of dispase II to potentiate cell extraction, we incubated neonatal or adult brain tissue with papain or collagenase II in combination with this enzyme. Data gathered indicate that dispase II can both potentiate and inhibit digestions, depending on enzyme combination and brain age

(Table 2). Moreover, dispase II showed specific effects on the extraction yield and integrity of each subpopulation.

Regarding neonatal brain, dispase II improved papain digestion of total neural cells by 71 %, but this rise was associated to a more than two-fold increase in lethality. Moreover, dispase II did not enhanced papain extraction of microglia, astrocytes or lymphocytes in newborns, and decreased the yield of these cell populations when used in combination with collagenase II.

The effects of dispase II on adult tissue differ from those found in
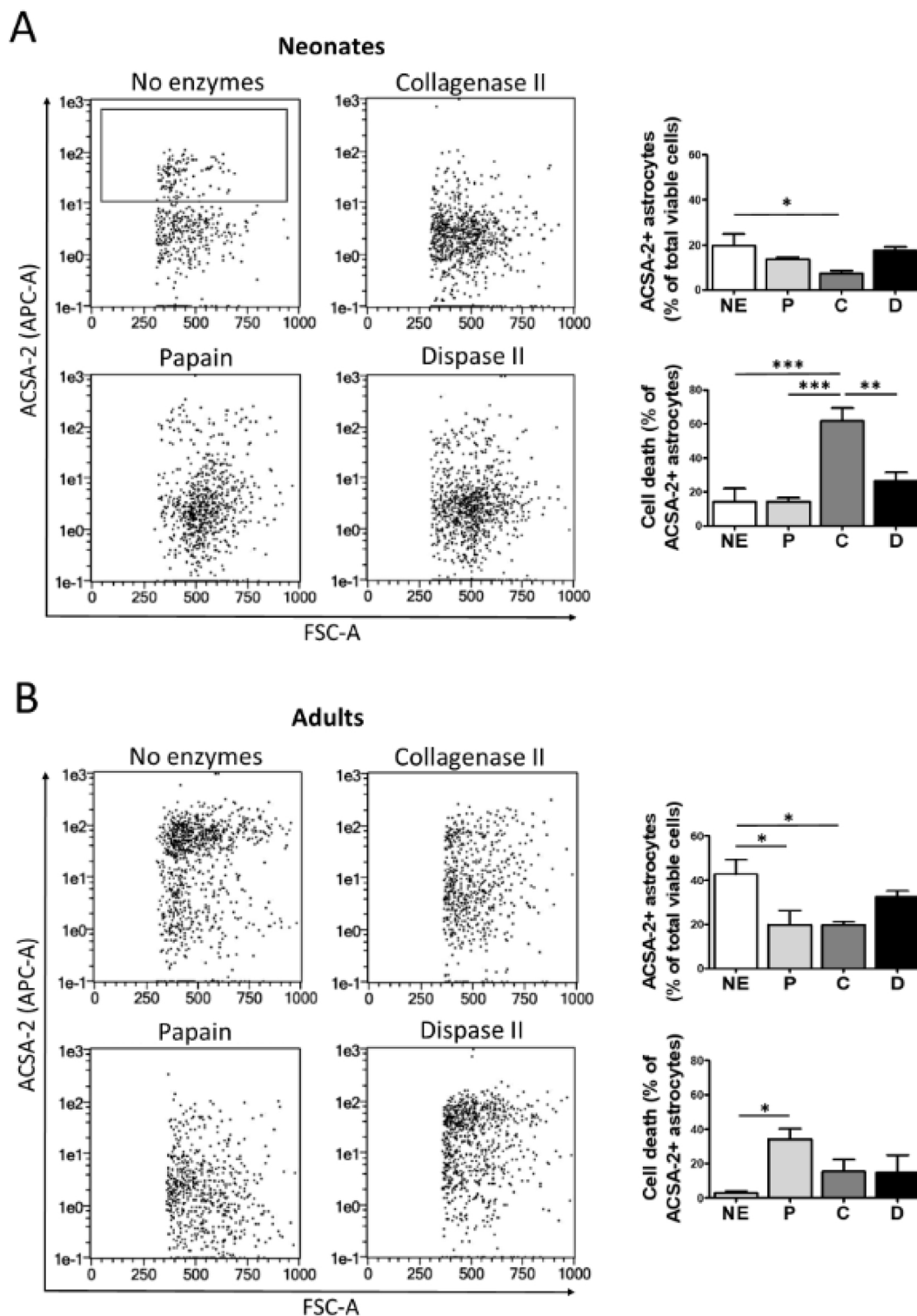
Fig. 6. Dissociation procedure for the extraction of astrocytes from neonatal and adult brain. Tissue from neonatal (A) and adult (B) brain was mechanically dissociated in the presence of papain (P), collagenase II (C), dispase II (D) or no enzymes (NE); and further purified through a 30 % Percoll gradient. Representative flow cytometry plots are shown. Astrocytes were identified as ACSA-2 + cells (gate). Cell death was measured after DAPI staining. Associated graphs correspond to % of astrocytes and astrocyte death. Data are expressed as mean ± S.E.M. (n = 3–4). *, p < 0.05; **, p < 0.01; ***, p < 0.001.

neonates, as we observed that dispase II enhances papain extraction of resting microglia (32 %) and lymphocytes (52 %); and raises total cell number when combined with collagenase II (25 %). Meanwhile, according to our analysis, extraction of adult astrocytes is negatively affected by dispase II since astrocyte viability significantly decreases when it is combined with either papain or collagenase II.

Summarizing, these results show that dispase II is useful to improve adult microglia extraction when combined with papain, whereas the impact of dispase II on astrocyte recovery is clearly negative at all ages.

Table 2

Effects of dispase II in combination with papain or collagenase II. Neonatal or adult brain tissue was dissociated with papain (P) or collagenase II (C) alone or in combination with dispase II (P + D and C + D). After 30 % Percoll gradient purification, cells obtained were stained with markers for resting microglia (CD11b +/CD45^{low}), lymphocytes (CD11b-/CD45+) and astrocytes (ACSA-2+/CD45-). Dead cells were also stained with DAPI. Cell number and viability were analyzed by flow cytometry. Values presented for P + D and C + D groups are presented as percentage change (100 x difference/original number) respect to papain or collagenase II digestion, respectively. Data correspond to mean ± S.E.M. (n = 4–6).

	Neonates		Adults	
	P + D	C + D	P + D	C + D
Total cell number per brain	**71.4 ± 9.1***	4.8 ± 0.3	12.0 ± 3.7	**24.9 ± 1.5****
Total cell death	**138.6 ± 31.3***	−7.8 ± 0.4	**69.2 ± 5.8****	**17.7 ± 0.9****
Resting microglia	1.8 ± 0.6	**−45.1 ± 13.3***	**32.6 ± 1.9****	38.3 ± 6.1
Resting microglia death	**291.4 ± 81.0***	83.0 ± 30.0	−3.5 ± 1.3	20.1 ± 4.6
Lymphocytes	39.7 ± 11.6	**−55.0 ± 10.3****	**52.2 ± 7.6***	135.1 ± 62.5
Astrocytes	24.8 ± 5.9	**−38.0 ± 7.5***	−14.6 ± 2.2	16.0 ± 4.5
Astrocyte death	**61.5 ± 9.3***	−25.2 ± 5.1	**38.8 ± 4.0***	**20.7 ± 1.5***

*p < 0.05 and **p < 0.01 *versus* papain or collagenase II alone.

3.7. Optimized dissociation procedure applied to evaluation of LPS effects in vivo

Despite optimal astrocyte isolation is achieved without enzymes, our comparative analysis revealed that the use of papain combined with dispase II is an appropriate choice to isolate a mixture of microglia and astrocytes from adult brain. Accordingly, this isolation protocol was further validated in a last set of experiments that examined the glial response to the inflammatory agent LPS in adult mice. For these experiments we selected a micro dose of LPS (i.p. injection, 0.5 mg/Kg) that does not cause mouse lethality and only induces a limited inflammatory response (Chen et al., 2012; Furube et al., 2018). After 3 days, brain cortex was extracted and processed for the analysis of resting microglia, activated microglia/macrophages and astrocytes by flow cytometry. Plots showed that LPS induces a statistically significant rise in the percentage of activated microglia/macrophages detected by its higher CD45 and CD11b staining intensity; while resting microglia decreases (Fig. 7A). Gating analysis showed a 2.8-fold increase in the activated microglia-macrophages/resting microglia ratio after LPS treatment. Interestingly, the number of ACSA-2+ astrocytes was also increased (Fig. 7B). Glial activation in these experiments was confirmed by fluorescent microscopy of brain sections using markers of microglia/macrophages and astrocytes such as Iba-1 and GFAP, respectively (Fig. 7C). Therefore, these observations indicate that the dissociation conditions used, based on papain and dispase II digestion, are suitable for quantitative evaluation of glial-cell reactivity in adult brain by flow cytometry, even when only mild inflammatory stimuli are applied.

4. Discussion

Our aim was to clarify which are the most appropriate dissociation conditions for simultaneous evaluation of brain microglia, astrocytes and lymphocytes by flow cytometry, distinguishing between neonatal and adult brain tissue. Few studies have compared the effectiveness of different dissociation methods on the extraction of brain cells (Legroux et al., 2015; de Haas et al., 2007); and, to our knowledge, no other studies have contrasted dissociation methodologies for the wide range of cell types analyzed here. Our approach highlights that microglia, astrocytes and lymphocytes have different requirements for optimal isolation and preservation; indicating that extraction protocols need to find a balance for all these cell types. Moreover, according to our comprehensive analysis, animal age has a heavy influence on the choice of appropriate dissociation conditions.

Microglia and astrocytes cultures are extensively used to examine cellular mechanisms dependent on glial cells (McCarthy and De Vellis, 1980) since, after astrocytes reach confluency, microglia can be efficiently separated by mild trypsinization and shaking (Saura et al., 2003; Moussaud and Draheim, 2010), magnetic separation (Bedi et al., 2013)

or immunopanning (Zhang et al., 2016). However, *in vitro* systems are unable to mimic the full functions performed by cells within the brain. An alternative tool used in our experiments is flow cytometry, which supplies fast quantitative data on cell number and viability of brain cell populations, avoiding many of the restrictions and experimental artefacts encountered by cell culture systems.

Nevertheless, samples processed for flow cytometry contain living cells. This implies that flow cytometry shares some of the limitations of cell cultures such as undesired cell activation during tissue extraction and staining. In fact, there is evidence that both microglia and astrocytes may be activated in response to stress during manipulation (Posel et al., 2016). In these cases, cell properties such as proliferation and release of pro- and anti-inflammatory factors may be altered; hindering the study of neuroinflammation. Regarding this potential problem, we generally detected less than 2 % of activated microglia in neonate extracts (1 % in adults) respect to total cells, suggesting that none of the enzymatic cocktails and Percoll gradients tested here trigger major cell activation.

Identification of microglia, macrophages and lymphocytes in our flow cytometry analysis was based on CD45 and CD11b expression, which is in accordance with previous studies (Legroux et al., 2015; Stevens et al., 2002; Ponomarev et al., 2005). However, a limitation of this approach is that activated microglia labelling overlaps with the staining of blood-born macrophages present in the brain, impairing clear distinction of these two populations (Bedi et al., 2013; Legroux et al., 2015). Complementary labelling with CD206 and CD38, expressed by subsets of activated microglia/macrophages (Hellström Erkenstam et al., 2016; Jablonski et al., 2015), helped to confirm that regions set for these populations and resting microglia in CD45/CD11b plots were properly placed. Meanwhile, the identity of lymphocytes gated in the same CD45/CD11b plots was further checked by CD3 stain of T cells (Schumak et al., 2015; Posel et al., 2016)

Contrarily to microglia and lymphocytes, few markers are available to identify astrocytes by flow cytometry. Traditional astrocyte markers such as GFAP or S100b, widely used for microscopy studies, have limited effectiveness in flow cytometry since intracellular antigen detection is often affected by cell fixation and permeabilization steps (Menon et al., 2014; Krutzik et al., 2005). Alternatively, astrocytes can be labelled for flow cytometry analysis with surface antigens ACSA-1 and ACSA-2. ACSA-1 recognizes the specific astrocyte glutamate-aspartate transporter GLAST (EAAT1) (Jungblut et al., 2012). However, it is only suitable for detection of neonatal astrocytes since GLAST is downregulated in most astrocytes as mice mature. According to microscopy studies, GLAST is restricted to the cerebellum, white matter regions and subgranular layer of the dentate gyrus in P25 mice (Furuta et al., 1997; Regan et al., 2007). Contrarily, ACSA-2 is a specific marker for both developing and adult astrocytes. The astrocyte glycoprotein ATP1B2, unique target identified for ACSA-2, shows a widespread
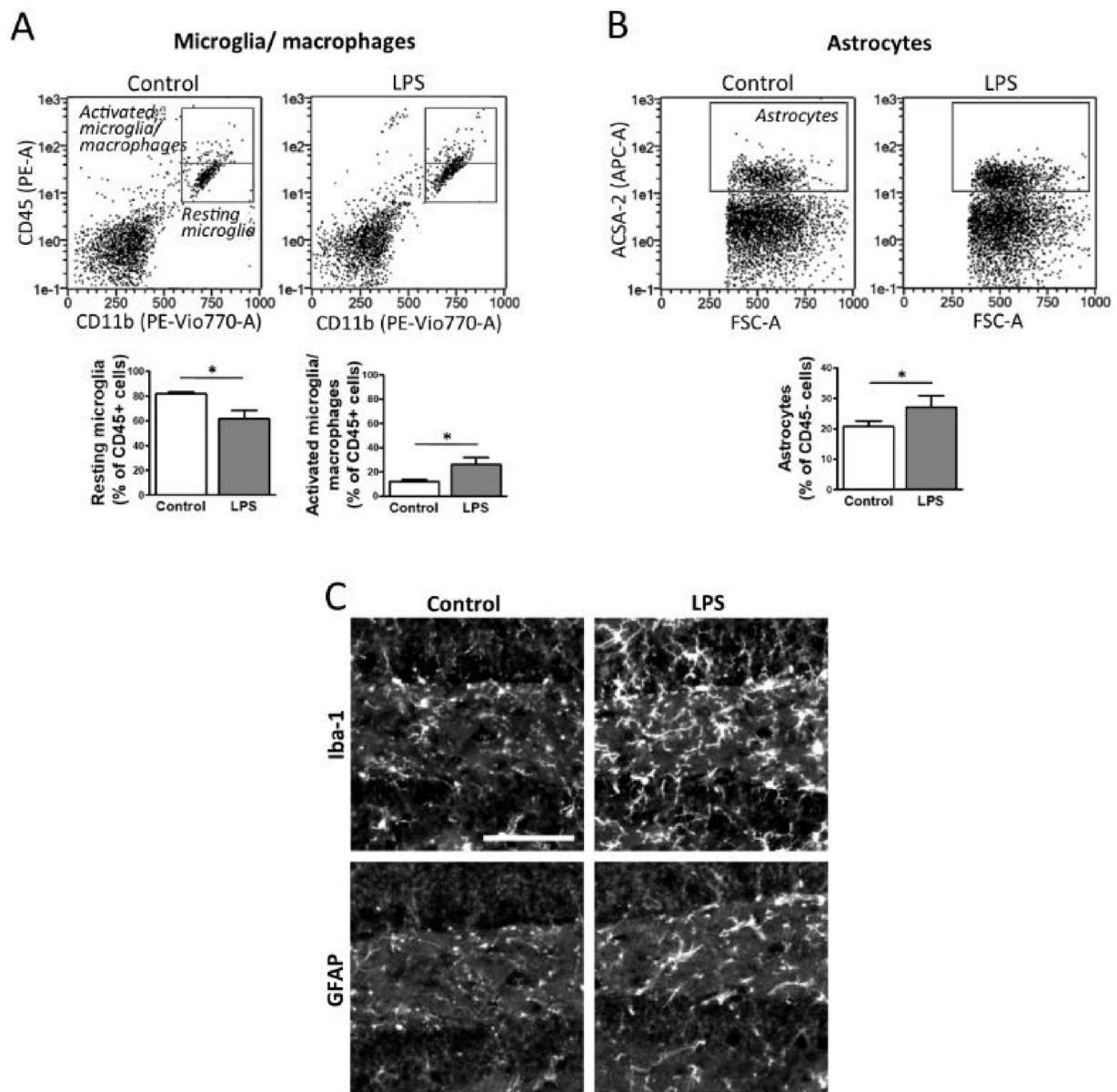
Fig. 7. Enzymatic isolation of brain cells with papain and dispase II to evaluate glia response to LPS. Animals were injected with LPS (0.5 mg/Kg, i.p.) to induce a mild inflammatory response. After 3 days, mice were sacrificed. Brain cells were isolated using papain and dispase II combined with gentle mechanical dissociation and DNase II incubation. Purification with 30 % Percoll was followed by flow cytometry analysis of (A) resting microglia (CD11b+/CD45^{low}) and activated microglia/macrophages (CD11b+/CD45^{high}), or (B) astrocytes (ACSA-2+/CD45-). Values are expressed as percentage of total CD45+ cells (A) or CD45-cells (B) and correspond to mean ± S.E.M. (n = 7–9). *, p < 0.05. (C) Another set of control and LPS-treated animals was fixed by perfusion, and brain sections stained for immunofluorescence detection of either Iba-1 or GFAP as markers of microglia and astrocytes, respectively. Representative images containing the dentate gyrus of hippocampus are shown (scale bar, 100 μm).

distribution within the developing brain and its expression is maintained in adults; including acute and chronic conditions associated to reactive astrogliosis (Batiuk et al., 2017). Moreover, we show here that ACSA-2 expression highly overlaps with ACSA-1 in neonatal brain astrocytes, in agreement with other authors (Kantzer et al., 2017). In consequence, ACSA-2 was our choice to label neonatal and adult astrocytes.

Multicolor flow cytometry has been useful to monitor the progression of inflammation in the CNS in several models of disease (Erturk et al., 2016; Ponomarev et al., 2005; Posel et al., 2016; Stevens et al., 2002). Here we quantified changes in the microglia and astrocyte activation state in response to a low LPS dose with the aim to evaluate if the methodology used here is suitable to detect subtle glial activation under mild inflammatory conditions. The LPS dose used in our

experiments (0.5 mg/Kg) is far from the LD$_{50}$ for LPS in mice (5−15 mg/kg) and did not caused any lethality (Chen et al., 2012; Furube et al., 2018). Despite this low dose, our methodology was able to detect an increase in the rate of activated/resting microglia in response to LPS; while Iba-1 immunostaining of brain sections confirmed cell cytometry data. In addition, the population of astrocytes identified as ACSA-2+ cells also responded to LPS; in agreement with the rise in GFAP immunoreactivity observed by microscopy. To our knowledge, these are the first observations that correlate astrocyte activation with ACSA-2 expression and support the use of ACSA-2 as a marker of astrocyte reactivity.

In our experiments, tissue was minced and incubated with enzymes at slow continuous rotation to favor homogenization. Alternatively, tissue fragmentation can be achieved by intermittent shaking (Schildge

et al., 2013; Singh et al., 2014). Dissociation protocols based on mechanical disruption, with no enzymatic incubation, have been widely used for the isolation of several cell types from brain of different mice ages (Bergmann et al., 1999; Ponomarev et al., 2005; Posel et al., 2016). In line with these authors, we observed better astrocyte recovery using mechanical dispersion, while enzymes generally harmed astrocytes. However, non-enzymatic digestion of both neonatal and adult brain generally results in a poor recovery of total cells, microglia and lymphocytes in comparison to the enzymatic treatments tested here. In line with these observations, many protocols for brain dissociation combine mechanical dissociation with enzymatic digestion (Posel et al., 2016; Pennartz et al., 2009; Ni and Aschner, 2010; Batiuk et al., 2017; Guttenplan and Liddelow, 2019). Furthermore, incubation with DNAse I was included in all dissociation conditions to eliminate DNA mucus that negatively affects cell viability (Posel et al., 2016).

Removal of myelin and cell debris after tissue digestion is critical not only for flow cytometry, but also for other downstream applications including the measurement of gene and protein expression. In this regard, Percoll density gradients are separation steps extensively used during isolation of brain and immune cells (Sedgwick et al., 1991; Lee and Tansey, 2013). The present study includes comparison of two alternative density gradients: 30 % and 30–70 %, finding a more than three-fold increase in the recovery of total cells with 30 % Percoll. Single gradients like this one primarily aim at efficient removal of myelin and debris. They are less time-consuming to set than multidensity gradients and avoid the difficulty of pipetting cells from layer interphases. In addition, we found generally higher viability among cells centrifuged in 30 % Percoll. Even though the Percoll gradient most frequently used for brain cell separation is 30-37-70 % (Cardona et al., 2006; Lee and Tansey, 2013; Sierra et al., 2007), our preference for 30 % Percoll is also supported by other authors (Legroux et al., 2015; Posel et al., 2016; Singh et al., 2014).

Regarding enzymatic digestion, our comparative analysis focuses on enzymes normally used for brain tissue dissociation: papain, collagenase II and dispase II. Although some studies use trypsin to digest brain (Bronstein et al., 2013; Saura et al., 2003; Schildge et al., 2013), there is evidence that this enzyme can activate glial cells as well as compromise viability (He et al., 2019; Singh et al., 2014). In consequence, trypsin was excluded from our study together with other enzymes rarely used for brain dissociation such as hyaluronidase or accutase (Erturk et al., 2016).

According to our data, papain combined with dispase II stands out for its efficiency to extract total neural cells from neonates (5.6 × 10^6 per brain) as well as resting microglia from adult brain (21 % of total cells). We also noticed that papain is generally less harmful for neonatal cells than other enzymes. In line with these observations, papain has been frequently used to isolate microglia from CNS (Moussaud and Draheim, 2010; Bruttger et al., 2015; Singh et al., 2014). On the contrary, our experiments indicate that papain is an enzyme particularly damaging for adult astrocytes, in agreement with other laboratories that have also reported adverse effects (Singh et al., 2014).

Regarding the neutral protease dispase II, we found that when used alone it behaves as a mild enzyme and yields dissociation values generally close to non-enzymatic digestion. However, when dispase II was used in combination with papain, we observed a significant increase in the number of total cells extracted from neonates as well as an improvement in the number of resting microglia and lymphocytes recovered from adults (32 % and 52 % respectively). However, our experiments also show that dispase II addition generally decreases the viability of cells extracted from both neonates and adults. Even so, our conclusion is that papain in combination with dispase II is the best choice to obtain resting microglia from adult brain. In agreement with these observations, papain and dispase II mixtures have been previously used to prepare primary cultures from adults (Lee and Tansey, 2013).

Although collagenase II is frequently used for the isolation of immune cells from the CNS (Erturk et al., 2016; Sedgwick et al., 1991; Sierra et al., 2007; Stevens et al., 2002), in our experiments digestion with this enzyme showed a poor recovery of total neural cells respect to other procedures, both in neonates and adults. However, even though the number of total cells extracted with collagenase II was low, it contained a high percentage of resting microglia, activated microglia/macrophages and lymphocytes in homogenates of all ages. This is in agreement with the preferential use of collagenase in other laboratories to isolate microglia (Mizee et al., 2017; Olah et al., 2012) and viable T cells (Smolders et al., 2013) from human brain. According to these authors, cell extracts obtained with collagenase-based methods followed by Percoll gradient purification are appropriate for flow cytometry analysis of different brain areas as well as for evaluation of disease conditions. On the contrary, collagenase II did not favor astrocyte recovery and caused a high lethality, especially in neonatal brain. Regarding dispase II, it has been previously used in association with collagenase II to digest adult brain (Cardona et al., 2006; Czupalla et al., 2018). However, we noticed a significant increase in cell death after dispase II addition associated to the raise in total cell number in adult homogenates. Moreover, dispase II decreased collagenase II extraction of all cell types in neonates.

In conclusion, we found that dissociation methods for neuroimmune cells are cell-type and mouse-age dependent, so that optimal protocols need to find a balance for the specific cell types targeted. Our comprehensive analysis has revealed that papain is an optimal choice for the simultaneous separation of brain microglia, astrocytes and infiltrated immune cells; whereas dispase II potentiates papain action only in adult tissue. Moreover, we found that optimized dissociation allows flow cytometry quantification of glial activation even when inflammatory stimuli are modest. Finally, non-enzymatic methods are the best choice when astrocytes are the only cell type isolated.

Authors contributions

PT and MF conceived the project. PT and BC designed the experiments. BC, FR and PT carried out the experiments. PT, BC and MF wrote the manuscript, and all authors proofread and approved it.

Conflicts of interest

The authors declare no conflict of interest.

Acknowledgements

References

Batiuk, M.Y., de Vin, F., Duque, S.I., Li, C., Saito, T., Saido, T., Fiers, M., Belgard, T.G., Holt, M.G., 2017. An immunoaffinity-based method for isolating ultrapure adult astrocytes based on ATP1B2 targeting by the ACSA-2 antibody. J. Biol. Chem. 292, 8874–8891. https://doi.org/10.1074/jbc.M116.765313.

Bedi, S.S., Smith, P., Hetz, R.A., Xue, H., Cox, C.S., 2013. Immunomagnetic enrichment and flow cytometric characterization of mouse microglia. J. Neurosci. Methods 219, 176–182. https://doi.org/10.1016/j.jneumeth.2013.07.017.

Ben-Gigi, L., Sweetat, S., Besser, E., Fellig, Y., Wiederhold, T., Polakiewicz, R.D., Behar, O., 2015. Astrogliosis induced by brain injury is regulated by Sema4B phosphorylation. eNeuro 2, 3. https://doi.org/10.1523/ENEURO.0078-14.2015.

Bergmann, C.C., Altman, J.D., Hinton, D., Stohlman, S.A., 1999. Inverted immunodominance and impaired cytolytic function of CD8+ T cells during viral persistence in the central nervous system. J. Immunol. 163, 3379–3387 doi: ji_v163n6p3379.

Boelen, E., Stassen, F.R., Steinbusch, H.W., Borchelt, D.R., Streit, W.J., 2012. Ex vivo cultures of microglia from young and aged rodent brain reveal age-related changes in microglial function. Neurobiol. Aging 33, 1. https://doi.org/10.1016/j.neurobiolaging.2010.05.008.

Bronstein, R., Torres, L., Nissen, J.C., Tsirka, S.E., 2013. Culturing microglia from the neonatal and adult central nervous system. J. Vis. Exp.(78), 50647. https://doi.org/

10.3791/50647.

Bruttger, J., Karram, K., Wortge, S., Regen, T., Marini, F., Hoppmann, N., Klein, M., Blank, T., Yona, S., Wolf, Y., Mack, M., Pinteaux, E., Muller, W., Zipp, F., Binder, H., Bopp, T., Prinz, M., Jung, S., Waisman, A., 2015. Genetic cell ablation reveals clusters of local self-renewing microglia in the mammalian central nervous system. Immunity 43, 92–106. https://doi.org/10.1016/j.immuni.2015.06.012.

Campanella, M., Sciorati, C., Tarozzo, G., Beltramo, M., 2002. Flow cytometric analysis of inflammatory cells in ischemic rat brain. Stroke 33, 586–592. https://doi.org/10.1161/hs0202.103399.

Cardona, A.E., Huang, D., Sasse, M.E., Ransohoff, R.M., 2006. Isolation of murine microglial cells for RNA analysis or flow cytometry. Nat. Protoc. 1, 1947.

Chen, Z., Jalabi, W., Shpargel, K.B., Farabaugh, K.T., Dutta, R., Yin, X., Kidd, G.J., Bergmann, C.C., Stohlman, S.A., Trapp, B.D., 2012. Lipopolysaccharide-induced microglial activation and neuroprotection against experimental brain injury is independent of hematogenous TLR4. J. Neurosci. 32, 11706–11715. https://doi.org/10.1523/JNEUROSCI.0730-12.2012.

Czupalla, C.J., Yousef, H., Wyss-Coray, T., Butcher, E.C., 2018. Collagenase-based single cell isolation of primary murine brain endothelial cells using flow cytometry. Bio-Protocol 8, 22. https://doi.org/10.21769/BioProtoc.3092.

de Haas, A.H., Boddeke, H.W., Brouwer, N., Biber, K., 2007. Optimized isolation enables ex vivo analysis of microglia from various central nervous system regions. Glia 55, 1374–1384. https://doi.org/10.1002/glia.20554.

Erturk, A., Mentz, S., Stout, E.E., Hedehus, M., Dominguez, S.L., Neumaier, L., Krammer, F., Llovera, G., Srinivasan, K., Hansen, D.V., Liesz, A., Scearce-Levie, K.A., Sheng, M., 2016. Interfering with the chronic immune response rescues chronic degeneration after traumatic brain injury. J. Neurosci. 36, 9962–9975. https://doi.org/10.1523/JNEUROSCI.1898-15.2016.

Furube, E., Kawai, S., Inagaki, H., Takagi, S., Miyata, S., 2018. Brain region-dependent heterogeneity and dose-dependent difference in transient microglia population increase during lipopolysaccharide-induced inflammation. Sci. Rep. 8https://doi.org/10.1038/s41598-018-20643-3. 2203-018-20643-3.

Furuta, A., Rothstein, J.D., Martin, L.J., 1997. Glutamate transporter protein subtypes are expressed differentially during rat CNS development. J. Neurosci. 17, 8363–8375.

Gordon, K.M., Duckett, L., Daul, B., Petrie, H.T., 2003. A simple method for detecting up to five immunofluorescent parameters together with DNA staining for cell cycle or viability on a benchtop flow cytometer. J. Immunol. Methods 275, 113–121 doi: S0022175903000097.

Guez-Barber, D., Fanous, S., Harvey, B.K., Zhang, Y., Lehrmann, E., Becker, K.G., Picciotto, M.R., Hope, B.T., 2012. FACS purification of immunolabeled cell types from adult rat brain. J. Neurosci. Methods 203, 10–18. https://doi.org/10.1016/j.jneumeth.2011.08.045.

Guttenplan, K.A., Liddelow, S.A., 2019. Astrocytes and microglia: models and tools. J. Exp. Med. 216, 71–83. https://doi.org/10.1084/jem.20180200.

He, Y., Taylor, N., Bhattacharya, A., 2019. Isolation and culture of astrocytes from postnatal and adult mouse brains. Methods Mol.Biol. 1938, 37–47. https://doi.org/10.1007/978-1-4939-9068-9_3.

Hellström Erkenstam, N., Smith, P.L., Fleiss, B., Nair, S., Svedin, P., Wang, W., Boström, M., Gressens, P., Hagberg, H., Brown, K.L., 2016. Temporal characterization of microglia/macrophage phenotypes in a mouse model of neonatal hypoxic-ischemic brain injury. Front. Cell. Neurosci. 10, 286. https://doi.org/10.3389/fncel.2016.00286.

Holt, L.M., Stoyanof, S.T., Olsen, M.L., 2019. Magnetic cell sorting for in vivo and in vitro astrocyte, neuron, and microglia analysis. Curr. Protoc. Neurosci. 88, e71. https://doi.org/10.1002/cpns.71.

Jablonski, K.A., Amici, S.A., Webb, L.M., de Dios Ruiz-Rosado, J., Popovich, P.G., Partida-Sanchez, S., Guerau-de-Arellano, M., 2015. Novel markers to delineate murine M1 and M2 macrophages. PLoS One 10, e0145342. https://doi.org/10.1371/journal.pone.0145342.

Jungblut, M., Tiveron, M.C., Barral, S., Abrahamsen, B., Knobel, S., Pennartz, S., Schmitz, J., Perraut, M., Pfrieger, F.W., Stoffel, W., Cremer, H., Bosio, A., 2012. Isolation and characterization of living primary astroglial cells using the new GLAST-specific monoclonal antibody ACSA-1. Glia 60, 894–907. https://doi.org/10.1002/glia.22322.

Kantzer, C.G., Boutin, C., Herzig, I.D., Wittwer, C., Reiss, S., Tiveron, M.C., Drewes, J., Rockel, T.D., Ohlig, S., Ninkovic, J., Cremer, H., Pennartz, S., Jungblut, M., Bosio, A., 2017. Anti-ACSA-2 defines a novel monoclonal antibody for prospective isolation of living neonatal and adult astrocytes. Glia 65, 990–1004. https://doi.org/10.1002/glia.23140.

Krutzik, P.O., Clutter, M.R., Nolan, G.P., 2005. Coordinate analysis of murine immune cell surface markers and intracellular phosphoproteins by flow cytometry. J. Immunol. 175, 2357–2365. https://doi.org/10.4049/jimmunol.175.4.2357.

Lee, J., Tansey, M.G., 2013. Microglia isolation from adult mouse brain. Microglia. Springer, pp. 17–23. https://doi.org/10.1007/978-1-62703-520-0_3.

Legroux, L., Pittet, C.L., Beauseigle, D., Deblois, G., Prat, A., Arbour, N., 2015. An optimized method to process mouse CNS to simultaneously analyze neural cells and leukocytes by flow cytometry. J. Neurosci. Methods 247, 23–31. https://doi.org/10.1016/j.jneumeth.2015.03.021.

Maric, D., Barker, J.L., 2005. Fluorescence-based sorting of neural stem cells and progenitors. Curr. Protoc. Neurosci. https://doi.org/10.1002/0471142301.ns0318s33. Chapter 3: Unit 3.18.

Marques, C.P., Cheeran, M.C., Palmquist, J.M., Hu, S., Urban, S.L., Lokensgard, J.R., 2008. Prolonged microglial cell activation and lymphocyte infiltration following experimental herpes encephalitis. J. Immunol. 181, 6417–6426 doi: 181/9/6417.

McCarthy, K.D., De Vellis, J., 1980. Preparation of separate astroglial and oligodendroglial cell cultures from rat cerebral tissue. J. Cell Biol. 85, 890–902.

Menon, V., Thomas, R., Ghale, A.R., Reinhard, C., Pruszak, J., 2014. Flow cytometry protocols for surface and intracellular antigen analyses of neural cell types. JoVE 94, e52241. https://doi.org/10.3791/52241.

Mizee, M.R., Miedema, S.S., van der Poel, M., Schuurman, K.G., van Strien, M.E., Melief, J., Smolders, J., Hendrickx, D.A., Heutinck, K.M., Hamann, J., 2017. Isolation of primary microglia from the human post-mortem brain: effects of ante-and post-mortem variables. Acta Neuropathol. Commun. 5, 16. https://doi.org/10.1186/s40478-017-0418-8.

Moussaud, S., Draheim, H.J., 2010. A new method to isolate microglia from adult mice and culture them for an extended period of time. J. Neurosci. Methods 187, 243–253. https://doi.org/10.1016/j.jneumeth.2010.01.017.

Ni, M., Aschner, M., 2010. Neonatal rat primary microglia: isolation, culturing, and selected applications. Curr. Protoc. Toxicol. https://doi.org/10.1002/0471140856.tx1217s43. Chapter 12:Unit 12.17.

Olah, M., Raj, D., Brouwer, N., De Haas, A.H., Eggen, B.J., Den Dunnen, W.F., Biber, K.P., Boddeke, H.W., 2012. An optimized protocol for the acute isolation of human microglia from autopsy brain samples. Glia 60, 96–111. https://doi.org/10.1002/glia.21251.

Pennartz, S., Reiss, S., Biloune, R., Hasselmann, D., Bosio, A., 2009. Generation of single-cell suspensions from mouse neural tissue. J. Vis. Exp.(29). https://doi.org/10.3791/1267. pii: 1267.

Ponomarev, E.D., Shriver, L.P., Maresz, K., Dittel, B.N., 2005. Microglial cell activation and proliferation precedes the onset of CNS autoimmunity. J. Neurosci. Res. 81, 374–389. https://doi.org/10.1002/jnr.20488.

Posel, C., Moller, K., Boltze, J., Wagner, D.C., Weise, G., 2016. Isolation and flow cytometric analysis of immune cells from the ischemic mouse brain. J. Vis. Exp.(108), 53658. https://doi.org/10.3791/53658.

Regan, M.R., Huang, Y.H., Kim, Y.S., Dykes-Hoberg, M.I., Jin, L., Watkins, A.M., Bergles, D.E., Rothstein, J.D., 2007. Variations in promoter activity reveal a differential expression and physiology of glutamate transporters by glia in the developing and mature CNS. J. Neurosci. 27, 6607–6619 doi: 27/25/6607.

Saura, J., Tusell, J.M., Serratosa, J., 2003. High-yield isolation of murine microglia by mild trypsinization. Glia 44, 183–189. https://doi.org/10.1002/glia.10274.

Schildge, S., Bohrer, C., Beck, K., Schachtrup, C., 2013. Isolation and culture of mouse cortical astrocytes. J. Vis. Exp.(71). https://doi.org/10.3791/50079. pii: 50079.

Schumak, B., Klocke, K., Kuepper, J.M., Biswas, A., Djie-Maletz, A., Limmer, A., van Rooijen, N., Mack, M., Hoerauf, A., Dunay, I.R., 2015. Specific depletion of Ly6C(hi) inflammatory monocytes prevents immunopathology in experimental cerebral malaria. PLoS One 10, e0124080. https://doi.org/10.1371/journal.pone.0124080.

Sedgwick, J.D., Schwender, S., Imrich, H., Dorries, R., Butcher, G.W., ter Meulen, V., 1991. Isolation and direct characterization of resident microglial cells from the normal and inflamed central nervous system. Proc. Natl. Acad. Sci. U. S. A. 88, 7438–7442.

Serrano-Perez, M.C., Martin, E.D., Vaquero, C.F., Azcoitia, I., Calvo, S., Cano, E., Tranque, P., 2011. Response of transcription factor NFATc3 to excitotoxic and traumatic brain insults: identification of a subpopulation of reactive astrocytes. Glia 59, 94–107. https://doi.org/10.1002/glia.21079.

Sierra, A., Gottfried-Blackmore, A.C., McEwen, B.S., Bulloch, K., 2007. Microglia derived from aging mice exhibit an altered inflammatory profile. Glia 55, 412–424. https://doi.org/10.1002/glia.20468.

Singh, V., Mitra, S., Sharma, A.K., Gera, R., Ghosh, D., 2014. Isolation and characterization of microglia from adult mouse brain: selected applications for ex vivo evaluation of immunotoxicological alterations following in vivo xenobiotic exposure. Chem. Res. Toxicol. 27, 895–903. https://doi.org/10.1021/tx500046k.

Smolders, J., Remmerswaal, E.B., Schuurman, K.G., Melief, J., van Eden, C.G., van Lier, R.A., Huitinga, I., Hamann, J., 2013. Characteristics of differentiated CD8 and CD4 T cells present in the human brain. Acta Neuropathol. 126, 525–535. https://doi.org/10.1007/s00401-013-1155-0.

Stevens, S.L., Bao, J., Hollis, J., Lessov, N.S., Clark, W.M., Stenzel-Poore, M.P., 2002. The use of flow cytometry to evaluate temporal changes in inflammatory cells following focal cerebral ischemia in mice. Brain Res. 932, 110–119.

Swartzlander, D.B., Propson, N.E., Roy, E.R., Saito, T., Saido, T., Wang, B., Zheng, H., 2018. Concurrent cell type-specific isolation and profiling of mouse brains in inflammation and Alzheimer's disease. JCI Insight 3. https://doi.org/10.1172/jci.insight.121109.

Thorne, B., Wonnacott, S., Dunkley, P.R., 1991. Isolation of hippocampal synaptosomes on Percoll gradients: cholinergic markers and ligand binding sites. J. Neurochem. 56, 479–484.

Zhang, Y., Sloan, S.A., Clarke, L.E., Caneda, C., Plaza, C.A., Blumenthal, P.D., Vogel, H., Steinberg, G.K., Edwards, M.S., Li, G., Duncan 3rd, J.A., Cheshier, S.H., Shuer, L.M., Chang, E.F., Grant, G.A., Gephart, M.G., Barres, B.A., 2016. Purification and characterization of progenitor and mature human astrocytes reveals transcriptional and functional differences with mouse. Neuron 89, 37–53. https://doi.org/10.1016/j.neuron.2015.11.013.